International Journal of Biological Macromolecules 263 (2024) 130319

Contents lists available at ScienceDirect

International Journal of Biological Macromolecules

journal homepage: www.elsevier.com/locate/ijbiomac

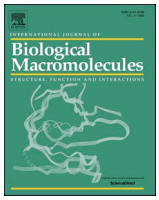

Pickering emulsions of thyme oil in water using oxidized cellulose nanofibers: Towards bio-based active packaging

Roberto J. Aguado [a,b,*], Elena Saguer [b], Núria Fiol [b], Quim Tarrés [a,b], Marc Delgado-Aguilar [a,b]

[a] LEPAMAP-PRODIS research group, University of Girona, C/ Maria Aurèlia Capmany, 61, 17003 Girona, Spain
[b] Department of Chemical and Agricultural Engineering and Agrifood Technology, University of Girona, C/ Maria Aurèlia Capmany, 61, 17003 Girona, Spain

ARTICLE INFO

Keywords:
Active food packaging
Cellulose nanofibers
Thyme essential oil

ABSTRACT

The antioxidant and antimicrobial properties of thyme essential oil (TEO) are useful for active food packaging, but its poor aqueous solubility restricts its applications. This work involves anionic cellulose nanofibers (CNFs) as the sole stabilizing agent for TEO-in-water emulsions, with oil concentrations ranging from 10 mL/L to 300 mL/L. A double mechanism was proposed: the adsorption of CNFs at oil/water interfaces restricted coalescence to a limited extent, while thickening (rheological stabilization) was required to avoid the buoyance of large droplets (>10 μm). Thickening effects comprised both higher viscosity (over 0.1 Pa·s at 10 s^{-1}) and yield stress (approximately 0.9 Pa). Dilute emulsions had good film-forming capabilities, whereas concentrated emulsions were suitable for paper coating. Regarding antimicrobial activity, CNF-stabilized TEO-in-water emulsions successfully inhibited the growth of both Gram-negative (*E. coli*, *S. typhimurium*) and Gram-positive bacteria (*L. monocytogenes*). As for the antioxidant properties, approximately 50 mg of paper or 3–5 mg of film per mL of food simulant D1 were required to attain 50 % inhibition in radical scavenging tests. Nonetheless, despite the stability and the active properties of these bio-based hydrocolloids, providing this antioxidant and antimicrobial activity was incompatible with maintaining the organoleptic properties of the foodstuff unaltered.

1. Introduction

In the techno-scientific literature, proposals for food packaging that involve nanocellulose have recently become a hot topic [1–4]. Even only considering one of the most popular kinds of nanocellulose, cellulose nanofibers (CNFs), their usage has been suggested for a myriad of applications. These include their role as support (films, nanopaper, nanocomposites), as barrier agent, as binder for other components, as carrier for drug delivery purposes, and as thickening agent, to name a few possibilities [5–7]. The choice of CNFs as Pickering stabilizer for water-immiscible liquids has also gained lots of interest, be it to generate food colloids for human intake [8,9] or to incorporate them into different kinds of packaging [10].

Water-immiscible liquids include many essential oils and plant extracts that, due to their antimicrobial and/or antioxidant activities, can offer protection to different kinds of foodstuff [11–13]. Mechanisms of protection may involve radical scavenging, *e.g.*, to prevent the chain reactions that lead to lipid oxidation in meat [14]. Other ways to protect the biomolecules in food products imply inhibiting microbial growth [15]. Limiting the proliferation of foodborne pathogens helps extend the shelf life of food and prevents worrisome infections such as listeriosis, cyclosporiasis, and salmonellosis [16].

There are many examples of successful emulsions of essential oils in water using nanocellulose as stabilizing agent: clove oil, emulsified with cellulose nanocrystals [17]; cinnamon essential oil, emulsified with CNFs [12]; citronella essential oil, using CNFs and chitosan, and [18] tea tree essential oil, stabilized by CNFs [19], to cite a few. The high stability of the resulting systems gives way to important industrial applications. In terms of food packaging, avoiding the use of organic solvents is key in coating operations, either on paper or directly on food [20]. It also grants more safety in the manufacturing process of any packaging material that involves solvent evaporation.

Thyme essential oil (TEO) has already been suggested for active food packaging [21], even in nanocellulose-supported films [22]. Its simultaneous antimicrobial and antioxidant activity, its high availability, and its consideration as safe for human consumption [23] justify the choice.

Abbreviations: CNFs, cellulose nanofibers; DPPH, 1,1-diphenyl-2-picrylhydrazyl; MH, Müller-Hinton; SEM, scanning electron microscopy; TEMPO, 2,2,6,6-tetramethylpiperidine-1-oxyl; TEO, thyme essential oil.

* Corresponding author at: LEPAMAP-PRODIS research group, University of Girona, C/ Maria Aurèlia Capmany, 61, 17003 Girona, Spain.
E-mail address: roberto.aguado@udg.edu (R.J. Aguado).

https://doi.org/10.1016/j.ijbiomac.2024.130319
Received 17 November 2023; Received in revised form 14 February 2024; Accepted 18 February 2024
Available online 21 February 2024

Nonetheless, to the best of our knowledge, its stabilization in aqueous media by means of CNFs is yet to be explored and evaluated. For that, the kind of functionalization is not trivial. A recent review article of ours deals with the role of electrostatic interactions in applications of nanocellulose such as thickening and emulsifying, also addressing how interrelated these two functions are [24]. In light of this, the regioselective oxidation of cellulose with 2,2,6,6-tetramethylpiperidine 1-oxyl radical (TEMPO) [25], followed by nanofibrillation, presents important advantages. Among them are the large surface area of the resulting CNFs, the high viscosity of their suspensions even at low concentration, and the effective repulsion within nanofibers [26]. The arguable lack of amphiphilicity of TEMPO-oxidized CNFs, given that they are even more hydrophilic than the original cellulose fibers, may be presented as a drawback. However, thymol, the main constituent of TEO, is a molecule with a permanent dipole (its phenolic –OH). Previous cases of success with water-immiscible polar liquids make us opt for TEMPO-oxidized nanofibers as stabilizing agent [27].

This work seeks to shed some light on the stabilization of TEO-in-water emulsions by means of TEMPO-oxidized nanofibers, then obtaining a proof of concept for their use in active food packaging by means of film forming and paper coating. To meet the first goal, the effects of TEO concentration and CNF concentration on emulsion stability were assessed, taking advantage of a hydrophobic dye. Insights were taken from droplet size (inspected by optical microscopy) and from the rheological properties of the emulsions. The activity of TEO/CNFs systems against three different strains of bacteria was visualized. Furthermore, TEO/CNF-containing films and packaging paper sheets were characterized in terms of scanning electron microscopy (SEM), migration, and radical scavenging capabilities, following immersion in food simulant D1.

2. Experimental

2.1. Materials

The packaging paper substrate to be coated was TSL testliner from SAICA (Zaragoza, Spain). Nanocellulose was produced from a bleached kraft eucalyptus pulp of industrial origin. All references to "water" in this section correspond to distilled water with an electrical conductivity of 2–6 μS/cm and a total content of solids below 10 mg/L.

TEO, Tween 80, Müller-Hinton (MH) agar, TEMPO, sodium alginate, and 1,1-diphenyl-2-picrylhydrazyl radical (DPPH) were purchased from Sigma-Aldrich (Barcelona, Spain). A hydrophobic dye, Red Conasol® 111, was provided by Proquimac PFC (Vacarisses, Spain). Folin-Ciocalteu reagent, Na_2CO_3, NaBr, NaClO, NaOH, KNO_3, gallic acid, and absolute ethanol were bought from Scharlab (Sentmenat, Spain).

Non-pathogenic strains of *Salmonella enterica*, subsp. *enterica serovar typhimurium* str. LT2 (CECT722) — henceforth *S. typhimurium* —, and *Listeria monocytogenes* (CECT4031) were supplied by the Spanish Type Culture Collection (Science Park of University of Valencia, Paterna, Spain) while *Escherichia coli* (ATCC10536) was obtained from the American Type Culture Collection (Manasas, VA, USA).

2.2. Oxidation and nanofibrillation

The bleached kraft eucalyptus pulp was diluted to 15 g/L and stirred at 3000 rpm for 10 min in a pulp disintegrator from IDM (Donostia-San Sebastian, Spain), in accordance with the ISO standard 5263 [28]. The resulting slurry was mixed with NaBr (0.100 g per gram of pulp, on a dry weight basis) and TEMPO (0.016 g/g pulp). Once dissolution was observed, 15 mmol of NaClO were added per gram of dry pulp. The suspension was diluted to 10 g/L, the temperature was kept at 23 °C and agitation was performed by means of a mechanical overhead stirrer (400–600 rpm). A 0.5 M NaOH solution was periodically added to maintain the pH in the 10–10.5 range. Oxidation was deemed finished when the pH remained stable at 10–10.5. TEMPO-oxidized cellulose was vacuum-filtered, thoroughly washed with distilled water.

Fibrillation of a TEMPO-oxidized cellulose suspension (12 g/L) towards CNFs was carried out with an NS1001L2K high-pressure homogenizer (HPH) from GEA Niro Soavi (Parma, Italy). The slurry was passed 3 times at 300 bar, 3 times at 600 bar, and 3 times at 900 bar. The characterization of the resulting CNFs, as described in previous works [25], yielded a cationic demand of (1.96 ± 0.10) meq/g and a carboxyl group content of (1.40 ± 0.10) mmol/g. The yield of nanofibrillation, understood in gravimetric terms [29], was >95 %. The transmittance at 600 nm of a dilute suspension (1 g/L) was 94.7 %.

2.3. Pickering emulsions

Heterogeneous mixtures comprising TEO (1–30 mL), TO-CNFs (0.0–1.0 g, on the basis of their dry weight), and enough water to make up to 100 mL were disaggregated by means of an UltraTurrax T25 device from IKA®-Werke GmbH (Staufen, Germany). The diameter of the rotor was 25 mm, the angular speed was set at 6400 rpm, and agitation was stopped after 2 min. Table 1 encompasses all the samples produced this way, indicating those that were used for film forming or paper coating.

To better visualize phase separation, 7 mg of Red Conasol® 111 were added to each emulsion or pseudo-emulsion. This step was only performed in those samples designated to assess nanocellulose-mediated stabilization. It was omitted for samples involving spectrophotometric measurements or any other kind of characterization. Some of the dyed emulsions were photographed in a LED-illuminated light box (20 W, neutral white) whose surface luminance was 310 cd/m^2.

2.4. Film forming and paper coating

Films were prepared from the emulsions by solvent evaporation, on polystyrene Petri dishes held at 23 °C for 48 h. For this purpose, only emulsions whose proportion of oil was 10 mL/L were chosen, since higher oil concentrations resulted in poor film formation. Four films were prepared from each formulation (T10/C6, T10/C8, and T10/C10).

An A4-sized piece of testliner was placed on a K Control Coater from RK Print Coat Instruments (Litlington, United Kingdom). The speed was set at 3 m/min and a total of 5 mL of emulsion was applied per sheet by using a smooth roll. Each emulsion (T100/C6, T100/C8, and T100/C10) was applied over four sheets. Additionally, judging that TEO/CNF layers were insufficient to grant proper barrier properties towards air, a bilayer coating operation was performed on packaging paper with: i) one first layer of sodium alginate (10 g/L) and CNFs (6 g/L); ii) a second layer of T100/C6.

Samples of known mass from the aforementioned films and papers, both with and without essential oil, were placed in ethanol/water

Table 1
Preparation of TEO-in-water emulsions and their coding. Although all of them were assessed in terms of phase separation, those used for film forming (a) and paper coating (b) are signaled.

	TEO (mL/L)				
CNFs (g/L)	10	50	100	200	300
0	T10/C0	–	–	–	–
1	T10/C1	T50/C1	T100/C1	T200/C1	T300/C1
2	T10/C2	T50/C2	T100/C2	T200/C2	T300/C2
3	T10/C3	T50/C3	T100/C3	T200/C3	T300/C3
4	T10/C4	T50/C4	T100/C4	T200/C4	T300/C4
5	T10/C5	T50/C5	T100/C5	T200/C5	T300/C5
6	T10/C6[a]	T50/C6	T100/C6[b]	T200/C6	T300/C6
7	T10/C7	T50/C7	T100/C7	T200/C7	T300/C7
8	T10/C8[a]	T50/C8	T100/C8[b]	T200/C8	T300/C8
10	T10/C10[a]	T50/C10	T100/C10[b]	T200/C10	T300/C10

[a] Employed for film forming.
[b] Employed for paper coating.

(volume ratio 1:1), also known as food simulant D1, to assess the release of active compounds. Migration to the simulant took place in closed vials, involving approximately 100 mg of coated paper or 10 mg of film per mL of liquid, and at 23 °C for 24 h.

2.5. Characterization

2.5.1. Analysis of emulsions

A stable and macroscopically homogeneous emulsion, T100/C8 (Table 1), was visualized by optical microscopy, using a DMR-XA device from Leica (Wetzlar, Germany). Besides observing the sample under halogen illumination over clear field, images were also taken with polarized light over dark field.

The apparent viscosity of CNF-stabilized TEO-in-water emulsions was measured with an RVI-2 rheometer from PCI (Albacete, Spain). The effects of shear rate, CNF concentration, and TEO concentration on rheological behavior were assessed. Furthermore, for low shear rate values, from 0.015 s^{-1} to 0.2 s^{-1}, the shear stress of a CNF suspension (5 g/L) was measured at 20 °C to estimate the apparent yield stress. For that, a compact rheometer from Anton Paar (Graz, Austria), model MCR 302e, was used with the module for concentric cylinders.

Measurements of cationic demand (or negative surface charge density) were carried out for TEO and TEO/CNF mixtures at different ratios, by potentiometric back titration [25,30]. Briefly, a known mass of emulsion or TEO was mixed with 10 mL of PDADMAC 0.001 N (excess) and centrifuged at 3000 ×*g* for 60 min. Afterwards, an aliquot was taken from the supernatant and titrated with PES-Na 0.001 N, while monitoring the potential by means of a particle charge detector from BTG Instruments (Weßling, Germany), model PCD-06.

The ζ-potential of dilute emulsions at pH 6.5–7.5 was recorded with a Zetasizer NanoZS device from Malvern Panalytical (Malvern, United Kingdom), using folded capillary cells with gold electrodes. To minimize the influence of the different ionic strength [31], KNO_3 was added to all samples, consistently reaching a concentration of 0.01 M.

2.5.2. Antibacterial activity

The antibacterial activity against *E. coli*, *S. typhimurium*, and *L. monocytogenes* was assessed for TEO, CNF suspensions and emulsions (100 mL/L in TEO) by disk diffusion, drop diffusion and volatilization assays [15]. TEO was tested pure and diluted to 500 mL/L in distilled water with Tween 80 (5 g/L), after sterilization by filtration through a 0.45 μm membrane filter. In any case, plates containing MH agar were inoculated by spreading 100 μL of the target bacterial culture (*ca.* 10^6 CFU) on the surface of the agar medium. For the disk and drop diffusion assays, 3 μL of each tested sample were placed in the central part of the plate, on a sterile antibiotic test paper (Ref. 1468, Filtros Anoia, Barcelona, Spain) or directly on the culture medium, respectively. For the volatilization test, 3 μL of emulsion were placed on the lid and the plates with MH agar inverted on the lid. All plates were sealed off with Parafilm (Neenah, WI, USA) to prevent TEO vapor losses and incubated at 30 °C for 24 h. Tests were performed in duplicate.

Two kinds of photographs were taken: of the culture medium in each case, from the ocular lens of a Junior microscope from Carl Zeiss (Jena, Germany), and from the Petri dishes in the aforementioned light box.

2.5.3. Assays on paper and films

Certain basic properties of sheets and films that could be hypothetically enhanced by TEO and/or CNFs, other than antibacterial and antioxidant activities, were assessed to detect any possible improvement as passive container. First, the grammage or basis weight of all films and sheets calculated. Thickness was measured with a digital micrometer from Starrett (Athol, MA, USA).

Changes in the air permeability of materials were evaluated by the Gurley method, following the ISO standard 5636/5. Briefly, the time required for 100 cm^3 of air to pass through a 6.45 cm^2 cross-sectional area, driven by a pressure gradient of 1.22 kPa, was measured. Bendtsen roughness was determined by means of an instrument from Metrotec (Donostia-San Sebastian, Spain) that conforms to the ISO 8791-2 standard. Burst index was computed using a device from IDM (Donostia-San Sebastian, Spain) in compliance with the ISO standard 2759 [28].

2.5.4. Antioxidant activity and phenolic content of ethanol/water extracts

Although the radical scavenging assay with DPPH is currently not standardized, the procedure was similar to the ones reported elsewhere (Echegoyen & Nerín 2015). Briefly, a 0.2 mM stock solution of DPPH in absolute ethanol was prepared in the first place. Then, 2 mL thereof were mixed with up to 2 mL of ethanol/water extracts, using more simulant D1 to make up to 4 mL (if necessary), and kept away from light at 35 °C. After 30 min, the absorbance at 516 nm was computed using a Shimadzu spectrophotometer, model UV-1280. Negative control tests were carried out by performing an identical extraction with extracts from paper or CNF films without TEO.

For the total phenolic content test, 0.4 mL of sample were diluted with 7.6 mL of distilled water and mixed with 0.4 mL of the Folin-Ciocalteu reagent. Then, 0.6 mL of Na_2CO_3 1 M was added and the mixture was kept away from light and at 23 °C for 120 min. The absorbance at 750 nm was recorded with the aforementioned spectrophotometer. Negative control tests involved extracts from paper or films without TEO. Positive control tests were performed by replacing the sample with an aqueous-alcoholic (1,1, vol/vol) solution of gallic acid of concentration 0.5 mg/mL.

3. Results and discussion

3.1. Macroscopic aspects of TEO/CNF/water mixtures

Depending on the concentration of TEO and CNFs, heterogeneous mixtures thereof in an aqueous matrix were found to appear in four ways (Fig. 1): I) completely emulsified and stabilized viscous liquids; II) completely stabilized gel emulsions; III) an oil phase in the upper part and an emulsified phase at the bottom; IV) an oil phase in the upper part and a serum phase at the bottom, with a thin creaming layer (water, oil, and CNFs) in between. The latter case (IV) only happened in the cases of low CNF concentration (1 g/L–2 g/L) and high oil fraction. For CNF concentrations equal or greater than the critical concentration (2 g/L–6 g/L, depending on the proportion of oil), the whole mixture was effectively stabilized (cases III and IV). Fig. 1a classifies these cases in a phase diagram. Although phase separation was clear for the lowest concentration of CNFs (Fig. 1b), the line that separates macroscopically homogeneous emulsions is diffuse around the critical CNF concentration. That said, the observation of a thin layer of oil on the top (Fig. 1c, excluding T300/C5) should not be understood as phase separation driven by the difference in density. The height of this thin layer did not depend on the diameter of the container, and thus it should not be confused with creaming. It owed to the facts that the surface tension of TEO is lower than that of water [32] and that the work of adhesion was relatively small [33]. It became unnoticeable at CNF concentrations above 7 or 8 g/L, likely due to the effect of the yield stress [34].

Comparing these results with those observed for other oil-in-water Pickering emulsions, also employing highly charged anionic CNFs, the critical concentration of stabilizing agent required was relatively high. For instance, an emulsion of hexadecane (20 wt%) in water needed 1.5 g of CNFs per L of emulsion to attain macroscopic homogeneity [35]. The same concentration sufficed to stabilize olive oil (100 mL/L) in water [36]. Even cinnamon essential oil (30 wt%) was emulsified with a slightly lower concentration of CNFs (5 g/L) [12] than those required by a similar proportion of TEO (at least 6 g/L). The desorption energy (E_d) is directly proportional to the oil-water interfacial tension (*IFT*) [37,38]:

$$E_d = \pi R^2 \, ITF \, (1–\cos\theta)^2 \quad (1)$$

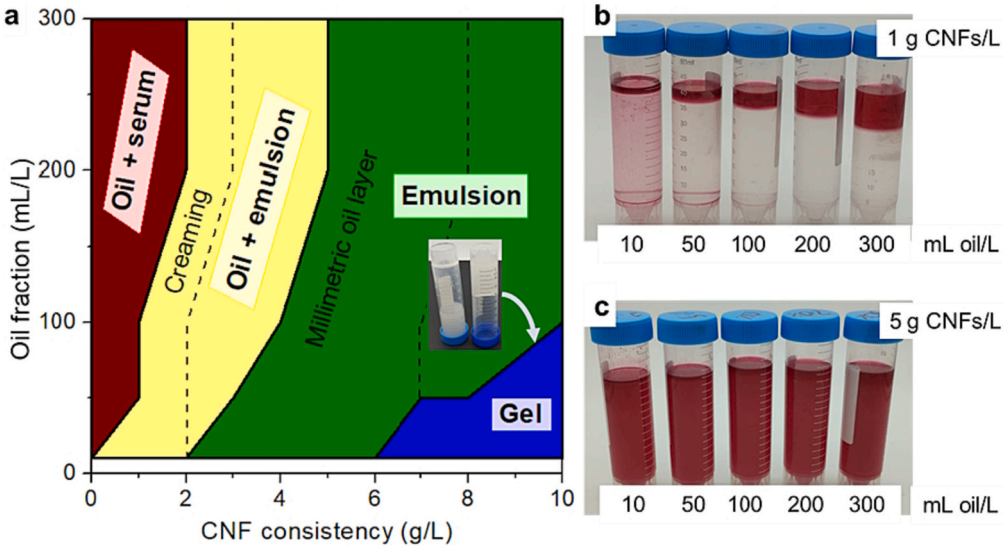

Fig. 1. Phase diagram elaborated from the naked-eye visual inspection of emulsions after 24 h (a), illustrated by pictures of dyed samples that correspond to T1–300/C1 (b) and T1–300/C5 (c). The inset image in (a) shows an example of gel behavior.

where R is the Sauter radius of the droplet and θ is the angle between the tangent to the oil/water interface and the tangent to the solid/water interface. Considering this, the stabilization of TEO was expected to require more CNFs than that of oils with high interfacial tension in water, such as alkanes, olive oil, and fish oil [39].

All mixtures comprising TEO and CNFs, including those with phase separation, remained highly stable (at least, macroscopically stable) in time once the first 24 h had passed. The volume occupied by each phase did not change significantly over at least four months of storage at room temperature.

Another important characteristic of Pickering emulsions was that increasing amounts of TEO disrupted gel behavior. The inset picture in Fig. 1a, taken from undyed samples with 7 g/L CNF concentration, shows that a nanocellulose suspension with 10 mL/L of TEO (T10/C7, right side) did not flow by gravity, but the emulsion adopted liquid flow by raising the percentage of oil to 100 g/L (T100/C7, left side).

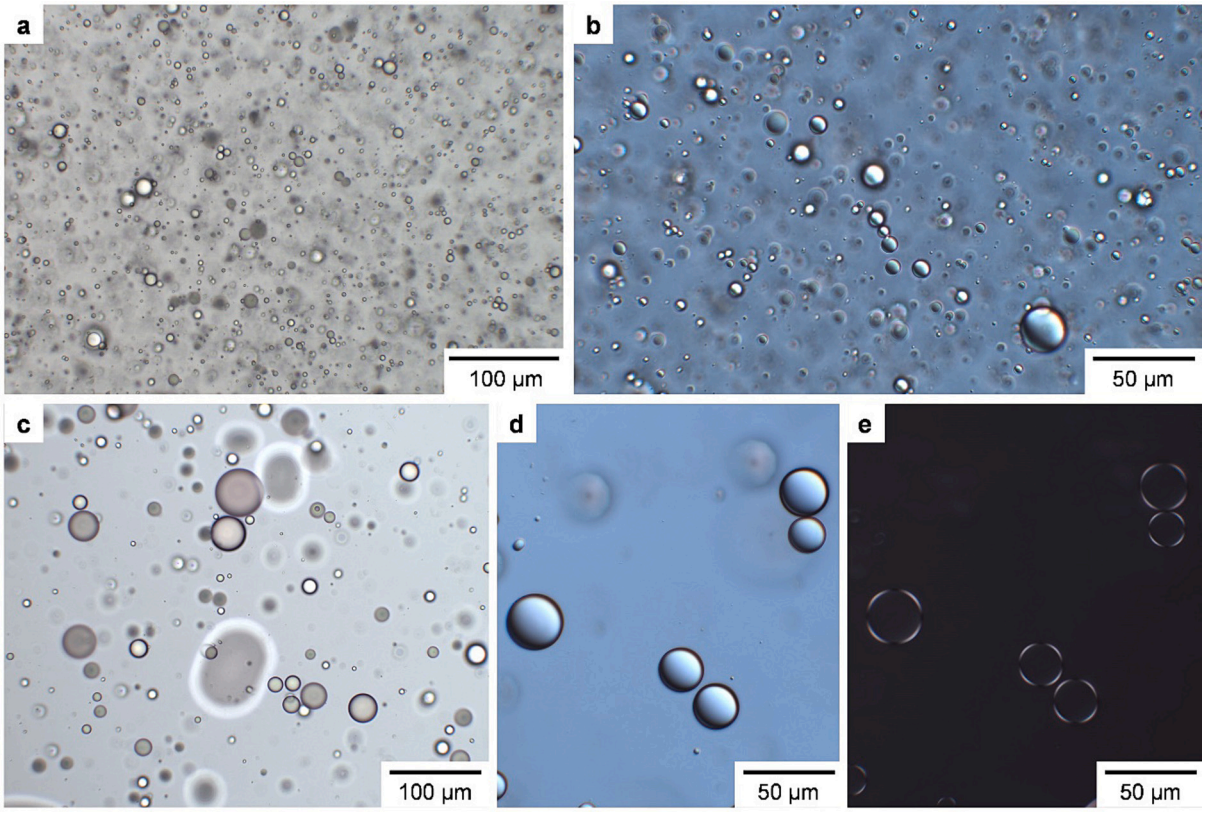

Fig. 2. Optical microscopy images of T100/C8, both freshly prepared (a, b) and after two weeks (c, d, e). Micrographs were taken under halogen illumination over clear field (a, c), using differential interference contrast (b, d), and under polarized light over dark field (e).

3.2. Assessment of stable Pickering emulsions

CNF-stabilized TEO-in-water emulsions were highly polydisperse in droplet size, as evidenced by the micrographs of Fig. 2 (T100/C8). There was evident coalescence of small droplets from freshly prepared emulsions (Fig. 2a, b) to those that accounted for 2 weeks of storage (Fig. 2c, d, e).

Besides the difference in droplet size, storage time had an appreciable effect, at least in qualitative terms, on surface coverage (towards more empty spaces), occurrence of multiplets (towards less of them), and droplet shape. 2-week-old emulsions, despite appearing homogeneous to the naked eye, contained some large (Feret's diameter > 25 μm), non-spherical drops [39] (Fig. 2c, behind the plane of focus).

Nonetheless, most droplets were spherical, with diverse diameters in the 0.5–20 μm range, and many examples of CNFs effectively preventing coalescence were detected. In Fig. 2c, the DLVO theory predicts that the small flocs of up to six droplets would merge in the absence or insufficiency of electrostatic repulsion [40]. Fig. 2d shows what appears to be a primary doublet at the upper part and a secondary doublet at the bottom. In both cases, the presence of CNFs at the water/oil interface avoided coalescence. In addition, the same part of the emulsion can be appreciated under polarized light in Fig. 2e. The optical activity of TEO droplets cannot be attributed to thymol, the main constituent of TEO, since it lacks chirality.

The chemical composition of this essential oil from Sigma-Aldrich has been accurately assessed elsewhere [41]. According to those results, although thymol is the main constituent (44.34 wt%), linalool and caryophyllene account for 4.81 wt% and 6.94 wt%, respectively. Each of these two compounds have an asymmetric carbon atom, which explains the optical activity appreciated in Fig. 2e. Indeed, Maltese crosses for linalool under polarized light have recently been reported [42].

Pickering emulsion is generally described according to one of these two mechanisms, if not to both: adsorption at the oil/water interface and rheological stabilization [24]. Indeed, this is a case in which both of them matter. On one hand, interactions of TEMPO-oxidized CNFs with both water and TEO prevented the collapse of primary doublets. A simple explanation based on amphiphilicity, by which the hydrophilic equatorial groups of CNFs interact with water and their hydrophobic axial planes interact with TEO, can satisfactorily describe why triglycerides and alkanes are emulsified with non-oxidized nanocellulose [43,44], but any temptation to apply it to this system should be avoided. In TEMPO-oxidized CNFs, the large hydration shells of carboxylate groups probably leave little area for dispersive forces on axial planes [45]. Instead, CNF-oil interactions are postulated to be the sum of i) these dispersive forces, ii) hydrogen bonding between the hydroxyl groups of some TEO constituents (such as thymol and linalool) and those of cellulose, and iii) ion-dipole interactions between the carboxylate groups of CNFs and the hydroxyl groups in TEO. Charge neutralization mechanisms are disregarded, since both TEO and CNFs had negative surface charge (Table S1).

It should be noted that, in terms of molecular mass transfer and in the presence of water, adsorption cannot be postulated to be stable. Although the surface carboxylate groups of CNFs are good H-bond acceptors and thymol is a relatively strong H-bond donor [46], water is still a better donor, more mobile, and more abundant in the medium. It is the additive effect of numerous interactions (dispersive, H-bonds, ion-dipole) over the surface of droplets, along with the enthalpic and entropic contributions of the hydrophobic effect [47], what can be translated into high enough desorption energies (Eq. (1)).

On the other hand, the electrostatic repulsion of CNFs at the oil/water interface does not suffice to explain stabilization, considering that the diameter of most droplets was >1 μm. If the continuous phase was only composed of water (Newtonian fluid, viscosity ~1 mPa·s at 20 °C), these droplets and their flocs would easily undergo buoyancy, leading to phase separation. In other words, gravitational effects would surpass Brownian motion [48]. However, TEMPO-oxidized CNFs, due to the retention of many water molecules in their hydration layers and to the repulsion between them, established a fibrillar network across the whole volume of the emulsion [48].

As displayed in Fig. 3, CNF-stabilized TEO-in-water had shear-thinning behavior, as commonly found for CNF suspensions [49,50]. Their viscosity at relatively low shear rate (3.5 s^{-1}) was 0.61 Pa·s if CNF concentration was 5 g/L or 5.0 Pa·s if CNF concentration was 10 g/L (Fig. 3a). In other words, they surpassed the viscosity of water by at least two orders of magnitude. Therefore, even the buoyant force experienced by a large oil drop is expected to meet high resistance to momentum transfer.

The shear stress registered at low shear rate (Fig. S1) allowed us to estimate the yield stress of CNF suspensions (5 g/L, enough to stabilize all emulsions except for T300/C5), as τ_0 = 0.9 Pa. The following empirical prediction of suspension stability was introduced by Darby [51]:

$$Y = \tau_0/[2\ R\ (\rho - \rho_{water})\ g] \quad (2)$$

where Y is the stability parameter, ρ is particle density, ρ_{water} is the density of water (~1000 kg/m^3), and g is the gravitational acceleration. Given the relatively low difference in density (83 kg/m^3), even drops that were in the millimeter range would remain suspended. This is one of the reasons why, despite the occurrence of coalescence, the volume of the emulsified phase did not significantly change over at least four months.

In TEO/CNFs/water systems, the only thickening agent was nanocellulose. However, although CNFs governed the rheological behavior of the emulsions, the oil exerted notorious effects on it. Consistently with the aforementioned disruption of gel behavior, its incorporation into CNF suspensions at 100 mL oil/L decreased their viscosity. Increasing that concentration to 200 mL/L or 300 mL/L resulted in further decrease

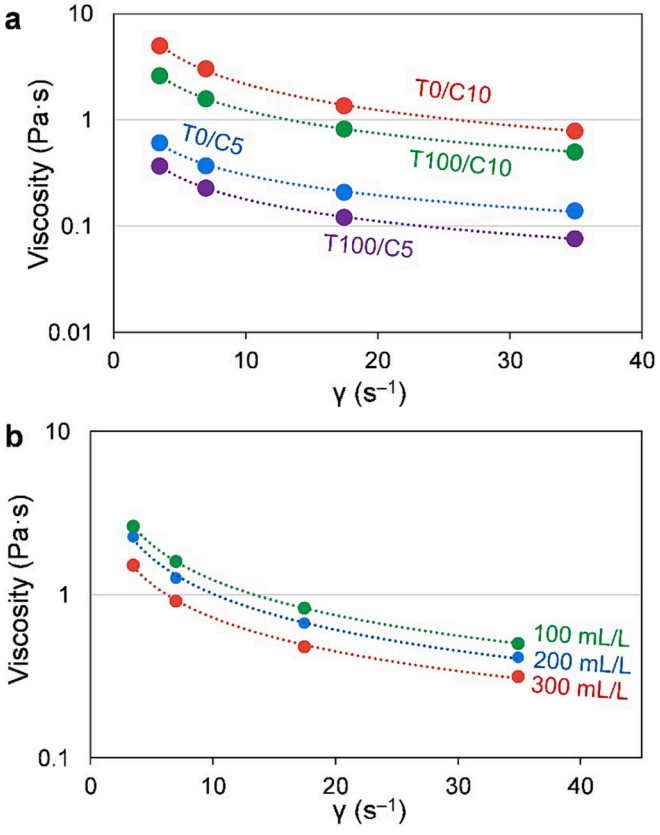

Fig. 3. Viscosity of CNF suspensions at 20 °C as a function of the shear rate (γ), highlighting the effect of incorporating 100 mL TEO/L (a) and the influence of its concentration in systems containing 10 g CNFs/L (b).

(Fig. 3b). Since TEO (33 mPa·s at 20 °C) was actually more viscous that water (1 mPa·s), the thinning phenomenon that it caused on aqueous CNF suspensions is further proof of TEO-CNF interactions. The viscosity of CNF suspensions has been suggested to follow a power function with the volume fraction of CNFs [52], but the adsorption of CNFs at water/oil interfaces reduced their effective volume in the system. In other words, TEO droplets partly captured CNFs, diminishing the effects of their large hydration shells on apparent viscosity.

3.3. Overview of films and coated paper sheets

T10/C8 displayed good film forming properties by simple solvent casting, not needing any additional film-forming agent. As shown in Fig. 4a, the film was easily lifted from the Petri dish, still visible below. Its SEM observation (Fig. 4b) revealed the persistence of the TEO droplets of the emulsion, no longer spherical in most cases. The removal of water decreased their resistance to deformation [53]. A few microfibers that resisted fibrillation can be distinguished, but the film mostly consisted of CNFs that, at least at these levels of magnification, appear as a continuous material. Finally, the inset figure, taken at the edge of the film and at higher magnification, highlights the shape of the protruding fibrils.

Regarding paper coating (Fig. 4c), the most noticeable difference between uncoated paper (Fig. 4d) and a sheet coated with T100/C6 (Fig. 4e) lied in surface porosity. The incorporation of CNFs, followed by drying, filled or closed down inter-fiber spaces and originated CNF-fiber hydrogen bonding [54,55]. Moreover, it was possible for TEO droplets and their constituents to become desorbed from CNFs and adsorbed onto the non-oxidized fibers of paper, which offered larger hydrophobic areas. Finally, bilayer coating, including sodium alginate/CNFs (6 g/L), further sealed the surface of liner papers (Fig. 4f, g).

Besides the active packaging properties that TEO conferred to packaging paper and CNF films, the specifications of any packaging material as passive container are always essential. As such, the testliner paper used in this work had important drawbacks in terms of barrier properties, should it be used for food packaging. Its hydrophilic and porous surface absorbed a drop of water placed on it and its air resistance was as low as 33 s/100 cm^3 (Table 2). The poor water resistance of conventional paper-based food packaging has been addressed in the literature, for instance, by using Pickering emulsions of alkenyl succinic anhydride [56].

Despite the low aqueous solubility of TEO, it is not a strongly hydrophobic essential oil, except for some constituents such as p-cymene. In any case, this relative hydrophobicity sufficed to retain a water drop on the surface of coated papers, at least for 20 s (Fig. S3). In addition, air resistance increased up to 157 s/100 cm^3 with T100/C10 and to 348 s/100 cm^3 with bilayer coating (Table 2). These specifications, although signifying a remarkable enhancement over the barrier properties of the original material, fall short of those of polyethylene-laminated paper. In another context, TEO/CNFs coatings also reduced the Bendtsen roughness of paper from 900 mL/min to 780 mL/min. Their effect on mechanical properties such as the burst index was non-significant.

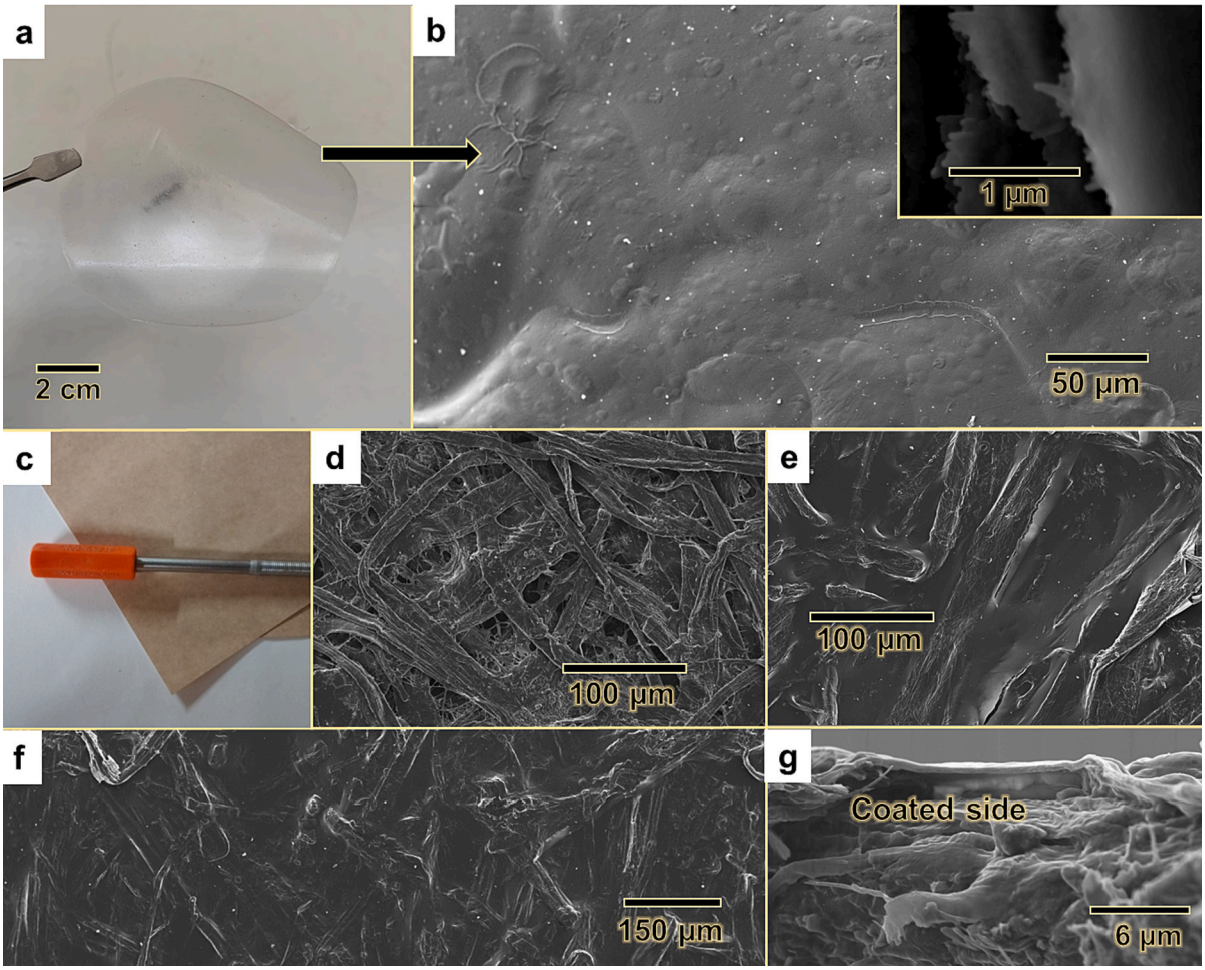

Fig. 4. Picture of a film formed from T100/C8 (a); SEM image from its surface (b), where the inset figure corresponds to the edge of the film; picture of coated paper (c); SEM images from the surface of uncoated paper (d), paper coated with T100/C6 (e), and paper coated with sodium alginate and T100/C6 (f); cross-section of the latter (g). The uncropped micrographs are available as Supplementary material (Fig. S2).

Table 2
Passive packaging properties of TEO/CNF films and coated or uncoated testliner sheets.

Material	Emulsion	Basis weight (g m^{-2})	Thickness (μm)	Burst index (kPa m^2 g^{-1})	Roughness (mL/min)	Air resistance (s/100 cm^3)
	T10/C6	20.1	17	3.2	700	
	T10/C8	21.0	25	3.5	700	
Film	T10/C10	21.2	23	3.2	780	>3600
Uncoated paper	None	170	226	2.0	900	33
	T100/C6	175	238	1.9	800	131
Paper (one layer)	T100/C8	176	239	2.1	780	150
	T100/C10	176	231	1.7	780	157
Paper (bilayer)	T100/C6	179	248	2.1	720	348

Unlike papers, TEO/CNF films were not permeable to air (air resistance > s/3600 cm^3). The air resistance of paper was only slightly enhanced because of its inherently rough and hydrophilic surface, while films were formed over a flat and water-resistant surface.

Their burst index was (3.3 ± 0.2) kPa m^2 g^{-1}, significantly above that of mechanical nanocellulose-starch films [57]. Their roughness was (730 ± 80) mL/min, their basis weight was (20.7 ± 0.8) g m^{-2}, and their thickness was (22 ± 5) μm (Table 2). Overall, films were highly flexible, strong, lightweight, thin, transparent, relatively smooth, and air-tight, but subject to the drawback of low moisture resistance. This is why other works employ hydrophobic bioplastics, such as poly(hydroxy alkanoates), as the matrix for nanocellulose-containing films [58].

3.4. Antioxidant and antimicrobial activity

CNF-only films, uncoated paper, CNF-coated paper (without TEO), and extracts thereof showed no significant radical scavenging activity against DPPH. Likewise, they did not inhibit the growth of any of the bacterial cultures tested. Hence, TEO was the only active component when it comes to both antioxidant and antimicrobial properties. Its IC50 against DPPH, under the conditions specified (ethanol/water, 9:1, vol), was estimated as 0.49 μL/mL or 0.45 mg/mL, slightly higher than that found for another thyme essential oil obtained by hydrodistillation [59]. Its total phenolic content was (246 ± 22) mg of gallic acid equivalent per g of oil. These results are mainly due to thymol, carvacrol, and linalool [41,60].

Ethanol/water (1:1, vol) extracts from coated papers and TEO/CNF films owed their antioxidant properties, indicated in Fig. 5 by the inhibition of the DPPH radical, to the release of TEO. CNF concentration (6–10 g/L), migration to food simulant D1 (Table S2), and radical scavenging activity appeared to be correlated, both in the case of films (Fig. 5a) and in the case of papers (Fig. 5b). In general, the lower the CNFs-to-TEO ratio, the more TEO was released to the food simulant D1 per unit of mass of film. This was expected, but it supports the thesis that any antioxidant activity that was appreciated was solely and directly exerted by released TEO. Preliminary experiments with water extracts did not attain significant DPPH inhibition, due to the poor aqueous solubility of TEO.

Gravimetric assays, corroborated by photometry at 280 nm, indicated that the migration of TEO from films to food simulant D1 was as high as 31 mg per dm^2 (Table S2). Although thymol is "recognized as a GRAS essential oil" by FDA [23] and approved as flavoring agent for "all categories of flavored foods" in the EU [61], non-flavored foods would see their organoleptic properties changed. Therefore, the application of the emulsions presented here may be limited to prepared food that includes thyme in the list of ingredients.

Regarding antibacterial activity, TEO strongly inhibited the growth of L. *monocytogenes* (Gram-positive), *E. coli* (Gram-negative), and *S. typhimurium* (Gram-negative) cultures. Proof of this can be found in pictures numbered "1" and "2" within Fig. 6. The inhibition effect on these microbes has already been proved for thymol [62–64]. This confirmation is highly valuable for food packaging applications, since these foodborne pathogens are the source of many concerns due to their resistance and ease to spread [64,65].

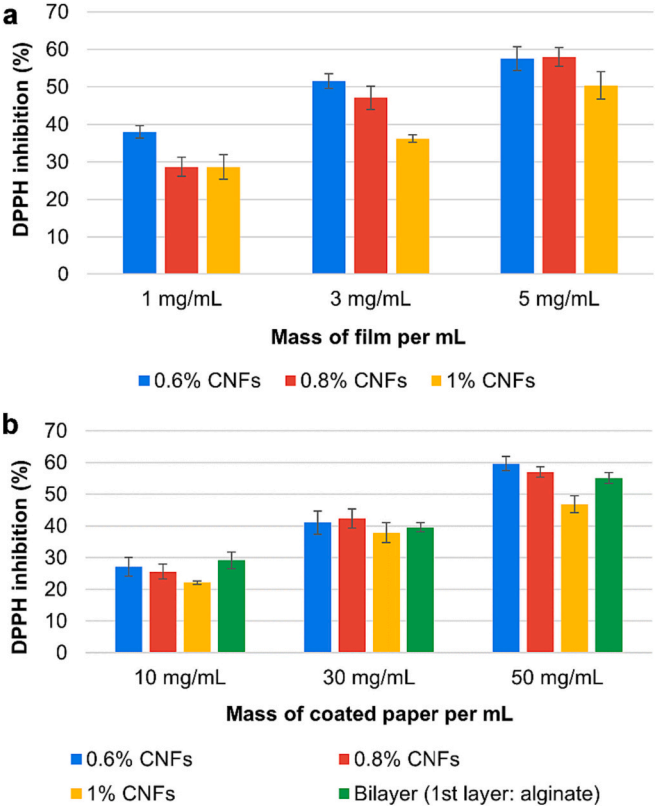

Fig. 5. Radical scavenging assays (on DPPH 0.1 mM) with the extracts from T10/C6, T10/C8 and T10/C10 films (a); extracts from paper sheets coated with T100/C6, T100/C8 and T100/C10 (b).

All three strains displayed growth over drops of CNF suspensions (Fig. 6a3, b3, c3), but not over drops of T100/C8 (Fig. 6a4, b4, c4). Although much smaller than for pure TEO or 50 vol% TEO, an inhibition halo was still appreciated around emulsion drops, at least in the cases of *E. coli* and *S. typhimurium*. When visualizing the samples at Fig. 6a4, b4, c4 by means of the Junior microscope, the difference between the medium outside of the emulsion (Fig. 6a5, b5, c5) and close to the edges of the drop (Fig. 6a6, b6, c6) was evident. No colonies of bacteria, either Gram-positive or Gram-negative, were identified at the area enclosed by the drop of emulsion, and growth was scarce in its vicinity. Finally, Fig. 6c7 shows the inhibition caused on *S. typhimurium* by the evaporation of TEO from an emulsion drop.

The inset images in Fig. 6 also indicate that the proliferation of *E. coli* and *L. monocytogenes* over the surface of films was avoided. However, unlike CNF-stabilized TEO-in-water emulsions, films displayed no inhibition halo. Release of TEO to aqueous agar media was negligible. Even the test for volatile agents against *S. typhimurium*, which resulted in effective inhibition when a drop of emulsion was left to undergo co-evaporation of water and TEO, had no appreciable effect with already

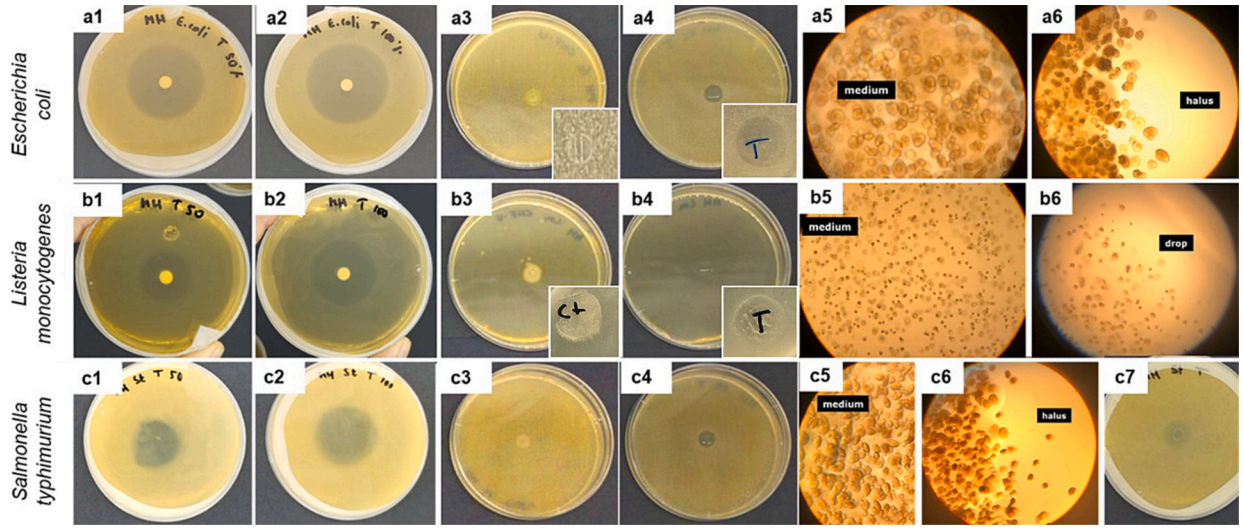

Fig. 6. Effects on the culture growth of *E. coli* (a), *L. monocytogenes* (b), and *S. typhimurium* (c). 1: TEO diluted to 50 vol% in water, using Tween 80 as surfactant; 2: non-diluted TEO; 3: drops of CNF suspensions; 4: drops of CNF-stabilized TEO-in-water emulsions; 5: visualization of bacterial colonies at the microscope; 6: inhibition of growth at the halo or by the drop of emulsion; *c7*: test for volatile agents against *S. typhimurium*. Inset pictures correspond to films made from the corresponding CNF suspensions (a3, b3) and TEO/CNF systems (a4, b4).

dried films or coated paper samples. During drying, large amounts of TEO evaporated along with water. Although the boiling point of thymol (232 °C) is much higher than that of water, their mixture greatly deviates from ideality [66]. Overall, the high activity coefficients that many essential oil constituents display in dilute aqueous systems results in higher volatility than what would be expected for ideal mixtures [67]. Nonetheless, the essential oil that remained in paper sheets and films after drying can be extracted by food simulant D1 and, in this sense, it is expected to be released to lipophilic contents.

4. Conclusions

Emulsions of TEO (10–300 mL/L) in water were long-term stabilized by CNFs (2–6 g/L). This stabilization is postulated to follow a double mechanism. On one hand, CNFs became adsorbed at oil-water interfaces, at least in the case of droplets with high Sauter radius. This did not fully prevent the coalescence of primary doublets, but it limited it enough to ensure macroscopical homogeneity. On the other hand, the diameter of most droplets was >1 μm, and thus rheological hindrance was necessary to prevent buoyancy. In fact, the dynamic viscosity at low shear rate of all stable, macroscopically homogeneous emulsions was at least two orders of magnitude over that of water. This, along with the yield stress provided by nanocellulose, allowed drops that were even larger than 20 μm in diameter to resist the buoyant force.

Coated papers and films, after reaching their equilibrium moisture, effectively worked as stable carriers of TEO. This advantage, the strong association between the hydrocolloid stabilizer and the bioactive compound, is also the source of an important limitation. Indeed, the lack of significant release to aqueous media, along with the fact that no spontaneous evaporation of TEO was appreciated, could restrict the use of CNF-stabilized TEO-in-water emulsions for active food packaging to lipophilic foodstuffs. Significant release (up to 31 mg dm^{-2} in 24 h) was attained with food simulant D1 (50 vol% ethanol).

TEO and CNF-stabilized TEO-in-water emulsions inhibited the growth of worrisome foodborne pathogens such as *L. monocytogenes*, *E. coli*, and *S. typhimurium*. Regarding the antioxidant activity, ethanol 50 vol% extracts required *ca.* 3 mg/mL of T10/C6 films or 50 mg of T100/C6-coated papers to attain 50 % inhibition of DPPH. As aforementioned, these active packaging features are subject to the release or migration of TEO. For instance, the packaging itself was protected from bacterial proliferation, but the lack of inhibition halo to aqueous agar media limits the potential protection of hydrophilic foodstuffs. Due to the requirement of release, attaining significant antioxidant or antimicrobial activity was deemed incompatible with keeping the organoleptic properties of the foodstuff unaltered. Hence, the TEO-in-water emulsions presented here are suggested for lipid-rich prepared food, with the packaging fulfilling the roles of emitter of bioactive compounds and flavor-release agent.

CRediT authorship contribution statement

Roberto J. Aguado: Writing – original draft, Methodology, Investigation, Formal analysis, Data curation, Conceptualization. **Elena Saguer:** Writing – review & editing, Visualization, Validation, Methodology, Investigation. **Núria Fiol:** Writing – review & editing, Visualization, Software, Resources, Formal analysis. **Quim Tarrés:** Writing – review & editing, Investigation, Data curation. **Marc Delgado-Aguilar:** Writing – review & editing, Visualization, Validation, Supervision, Resources, Project administration, Methodology, Funding acquisition, Conceptualization.

Declaration of competing interest

The authors declare that they have no known competing financial interests or personal relationships that could have appeared to influence the work reported in this paper.

Data availability

All data displayed in the article, as supplementary information, or else available upon request.

Acknowledgements

Authors wish to acknowledge the Spanish Ministry of Science and Innovation for the financial support to the project NextPack (PID2021-124766OA-I00). Marc Delgado-Aguilar and Quim Tarrés are Serra Húnter Fellows.

Appendix A. Supplementary data

Supplementary data to this article can be found online at https://doi.

org/10.1016/j.ijbiomac.2024.130319.

References

[1] M. Garrido-Romero, R. Aguado, A. Moral, C. Brindley, M. Ballesteros, From traditional paper to nanocomposite films: analysis of global research into cellulose for food packaging, Food Packag. Shelf Life 31 (2022) 100788, https://doi.org/10.1016/j.fpsl.2021.100788.

[2] A.K. Bharimalla, S.P. Deshmukh, N. Vigneshwaran, P.G. Patil, V. Prasad, Nanocellulose-polymer composites for applications in food packaging: current status, future prospects and challenges, Polym.-Plast. Technol. Eng. 56 (2017) 805–823, https://doi.org/10.1080/03602559.2016.1233281.

[3] S.S. Ahankari, A.R. Subhedar, S.S. Bhadauria, A. Dufresne, Nanocellulose in food packaging: a review, Carbohydr. Polym. 255 (2021) 117479, https://doi.org/10.1016/j.carbpol.2020.117479.

[4] G.R. Raghav, K.J. Nagarajan, M. Palaninatharaja, M. Karthic, R.A. Kumar, M. A. Ganesh, Reuse of used paper egg carton boxes as a source to produce hybrid AgNPs- carboxyl nanocellulose through bio-synthesis and its application in active food packaging, Int. J. Biol. Macromol. 249 (2023) 126119, https://doi.org/10.1016/j.ijbiomac.2023.126119.

[5] B. Bideau, E. Loranger, C. Daneault, Nanocellulose-polypyrrole-coated paperboard for food packaging application, Prog Org Coat 123 (2018) 128–133, https://doi.org/10.1016/j.porgcoat.2018.07.003.

[6] P. Tyagi, L. Pal, M. Hubbe, Effects of montmorillonite, kaolinite, protein, and AKD on nanocellulose-based barrier coatings for packaging, in: Paper Conference, Trade Show (Eds.), PaperCon 2017: Renew, Redefine the Future, Rethink, 2017, pp. 837–852. https://www.scopus.com/inward/record.uri?eid=2-s2.0-85041503833&partnerID=40&md5=c0e91999cc858638949641be2e144f03.

[7] F. Vilarinho, A.S. Silva, M.F. Vaz, J.P. Farinha, Nanocellulose in green food packaging, Crit. Rev. Food Sci. Nutr. 58 (2018) 1526–1537, https://doi.org/10.1080/10408398.2016.1270254.

[8] D. Parés, M. Àngels Pèlach, M. Toldrà, E. Saguer, Q. Tarrés, C. Carretero, Nanofibrillated cellulose as functional ingredient in emulsion-type meat products, Food Bioproc. Tech. 11 (2018) 1393–1401, https://doi.org/10.1007/s11947-018-2104-7.

[9] Q.-H. Chen, J. Zheng, Y.-T. Xu, S.-W. Yin, F. Liu, C.-H. Tang, Surface modification improves fabrication of Pickering high internal phase emulsions stabilized by cellulose nanocrystals, Food Hydrocoll. 75 (2018) 125–130, https://doi.org/10.1016/j.foodhyd.2017.09.005.

[10] Y. Zheng, H. Oguzlu, A. Baldelli, Y. Zhu, M. Song, A. Pratap-Singh, F. Jiang, Sprayable cellulose nanofibrils stabilized phase change material Pickering emulsion for spray coating application, Carbohydr. Polym. 291 (2022) 119583, https://doi.org/10.1016/j.carbpol.2022.119583.

[11] C. Li, M. Bai, X. Chen, W. Hu, H. Cui, L. Lin, Controlled release and antibacterial activity of nanofibers loaded with basil essential oil-encapsulated cationic liposomes against Listeria monocytogenes, Food Biosci. 46 (2022), https://doi.org/10.1016/j.fbio.2022.101578.

[12] A.G. de Souza, R.R. Ferreira, E.S.F. Aguilar, L. Zanata, D. dos S. Rosa, Cinnamon essential oil nanocellulose-based pickering emulsions: processing parameters effect on their formation, stabilization, and antimicrobial activity, Polysaccharides 2 (2021) 608–625, https://doi.org/10.3390/polysaccharides2030037.

[13] T. Mehdizadeh, H. Tajik, A.M. Langroodi, R. Molaei, A. Mahmoudian, Chitosan-starch film containing pomegranate peel extract and Thymus kotschyanus essential oil can prolong the shelf life of beef, Meat Sci. 163 (2020), https://doi.org/10.1016/j.meatsci.2020.108073.

[14] R. Domínguez, M. Pateiro, M. Gagaoua, F.J. Barba, W. Zhang, J.M. Lorenzo, A comprehensive review on lipid oxidation in meat and meat products, Antioxidants 8 (2019) 429, https://doi.org/10.3390/antiox8100429.

[15] E. Abdollahzadeh, A. Nematollahi, H. Hosseini, Composition of antimicrobial edible films and methods for assessing their antimicrobial activity: a review, Trends Food Sci. Technol. 110 (2021) 291–303, https://doi.org/10.1016/j.tifs.2021.01.084.

[16] A.J. Linscott, Food-Borne illnesses, Clin. Microbiol. Newsl. 33 (2011) 41–45, https://doi.org/10.1016/j.clinmicnews.2011.02.004.

[17] H. Yu, G. Huang, Y. Ma, Y. Liu, X. Huang, Q. Zheng, P. Yue, M. Yang, Cellulose nanocrystals based clove oil Pickering emulsion for enhanced antibacterial activity, Int. J. Biol. Macromol. 170 (2021) 24–32, https://doi.org/10.1016/j.ijbiomac.2020.12.027.

[18] S.S. Ibrahim, W.S. Abou-Elseoud, H.H. Elbehery, M.L. Hassan, Chitosan-cellulose nanoencapsulation systems for enhancing the insecticidal activity of citronella essential oil against the cotton leafworm Spodoptera littoralis, Ind. Crop. Prod. 184 (2022), https://doi.org/10.1016/j.indcrop.2022.115089.

[19] G. da S. Ferreira, D.J. da Silva, A.G. Souza, E.D.C. Yudice, I.B. de Campos, R.D. Col, A. Mourão, H.S. Martinho, D.S. Rosa, Eco-friendly and effective antimicrobial Melaleuca alternifolia essential oil Pickering emulsions stabilized with cellulose nanofibrils against bacteria and SARS-CoV-2, Int. J. Biol. Macromol. 243 (2023) 125228, https://doi.org/10.1016/j.ijbiomac.2023.125228.

[20] L. Qiu, M. Zhang, B. Chitrakar, B. Adhikari, C. Yang, Effects of nanoemulsion-based chicken bone gelatin-chitosan coatings with cinnamon essential oil and rosemary extract on the storage quality of ready-to-eat chicken patties, Food Packag. Shelf Life 34 (2022) 100933, https://doi.org/10.1016/j.fpsl.2022.100933.

[21] L. Zhou, M. Hao, T. Min, X. Bian, H. Du, X. Sun, Z. Zhu, Y. Wen, Kaolin incorporated with thyme essential oil for humidity-controlled antimicrobial food packaging, Food Packag. Shelf Life 38 (2023) 101106, https://doi.org/10.1016/j.fpsl.2023.101106.

[22] S. Casalini, M.G. Baschetti, M. Cappelletti, A.C. Guerreiro, C.M. Gago, S. Nici, M. D. Antunes, Antimicrobial activity of different nanocellulose films embedded with thyme, cinnamon, and oregano essential oils for active packaging application on raspberries, Front Sustain Food Syst 7 (2023), https://doi.org/10.3389/fsufs.2023.1190979.

[23] Federal Register, Thymol; Exemption From the Requirement of a Tolerance. https://www.federalregister.gov/documents/2022/09/07/2022-19294/thymol-exemption-from-the-requirement-of-a-tolerance, 2022. (Accessed 27 July 2023).

[24] R.J. Aguado, A. Mazega, Q. Tarrés, M. Delgado-Aguilar, The role of electrostatic interactions of anionic and cationic cellulose derivatives for industrial applications: a critical review, Ind Crops Prod 201 (2023) 116898, https://doi.org/10.1016/j.indcrop.2023.116898.

[25] A. Mazega, A.F. Santos, R. Aguado, Q. Tarrés, N. Fiol, M.À. Pèlach, M. Delgado-Aguilar, Kinetic study and real-time monitoring strategy for TEMPO-mediated oxidation of bleached eucalyptus fibers, Cellulose 30 (2023) 1421–1436, https://doi.org/10.1007/s10570-022-05013-7.

[26] S. Arola, Z. Kou, B.J.M. Rooijakkers, R. Velagapudi, M. Sammalkorpi, M.B. Linder, On the mechanism for the highly sensitive response of cellulose nanofiber hydrogels to the presence of ionic solutes, Cellulose 29 (2022) 6109–6121, https://doi.org/10.1007/s10570-022-04664-w.

[27] R.J. Aguado, A. Mazega, N. Fiol, Q. Tarrés, P. Mutjé, M. Delgado-Aguilar, Durable nanocellulose-stabilized emulsions of dithizone/chloroform in water for Hg2+ detection: a novel approach for a classical problem, ACS Appl. Mater. Interfaces (2023), https://doi.org/10.1021/acsami.2c22713.

[28] ISO, ISO TC/6: Paper, Board and Pulps, International Standardization Organization, Geneva (Switzerland), 2011.

[29] G. Signori-Iamin, A.F. Santos, M.L. Corazza, R. Aguado, Q. Tarrés, M. Delgado-Aguilar, Prediction of cellulose micro/nanofiber aspect ratio and yield of nanofibrillation using machine learning techniques, Cellulose (2022), https://doi.org/10.1007/s10570-022-04847-5.

[30] F. Serra-Parareda, R. Aguado, Q. Tarrés, P. Mutjé, M. Delgado-Aguilar, Potentiometric back titration as a robust and simple method for specific surface area estimation of lignocellulosic fibers, Cellulose 28 (2021) 10815–10825, https://doi.org/10.1007/s10570-021-04250-6.

[31] K. Heise, C. Jonkergouw, E. Anaya-Plaza, V. Guccini, T. Pääkkönen, M.B. Linder, E. Kontturi, M.A. Kostiainen, Electrolyte-controlled permeability in nanocellulose-stabilized emulsions, Adv. Mater. Interfaces 9 (2022) 2200943, https://doi.org/10.1002/admi.202200943.

[32] J.-H. Tak, M.B. Isman, Enhanced cuticular penetration as the mechanism of synergy for the major constituents of thyme essential oil in the cabbage looper, Trichoplusia ni, Ind Crops Prod 101 (2017) 29–35, https://doi.org/10.1016/j.indcrop.2017.03.003.

[33] C.J. van Oss, Chapter two-the apolar and polar properties of liquid water and other condensed-phase materials, in: C.J.B.T.-I.S, T. van Oss (Eds.), The Properties of Water and their Role in Colloidal and Biological Systems, Elsevier, 2008, pp. 13–30, https://doi.org/10.1016/S1573-4285(08)00202-0.

[34] L. Jørgensen, M. Le Merrer, H. Delanoë-Ayari, C. Barentin, Yield stress and elasticity influence on surface tension measurements, Soft Matter 11 (2015) 5111–5121, https://doi.org/10.1039/C5SM00569H.

[35] Y. Goi, S. Fujisawa, T. Saito, K. Yamane, K. Kuroda, A. Isogai, Dual functions of TEMPO-oxidized cellulose nanofibers in oil-in-water emulsions: a Pickering emulsifier and a unique dispersion stabilizer, Langmuir 35 (2019) 10920–10926, https://doi.org/10.1021/acs.langmuir.9b01977.

[36] J. Luo, K. Huang, X. Zhou, Y. Xu, Elucidation of oil-in-water emulsions stabilized with celery cellulose, Fuel 291 (2021) 120210, https://doi.org/10.1016/j.fuel.2021.120210.

[37] I. Capron, O.J. Rojas, R. Bordes, Behavior of nanocelluloses at interfaces, Curr Opin colloid, Interface Sci. 29 (2017) 83–95, https://doi.org/10.1016/j.cocis.2017.04.001.

[38] B.P. Binks, Emulsions — recent advances in understanding, in: B.P. Binks (Ed.), Modern Aspects of Emulsion Science, The Royal Society of Chemistry, Cambridge (U.K.), 1998, pp. 1–55, https://doi.org/10.1039/9781847551474-00001.

[39] Z. Li, D. Yu, Controlled ibuprofen release from Pickering emulsions stabilized by pH-responsive cellulose-based nanofibrils, Int. J. Biol. Macromol. 242 (2023) 124942, https://doi.org/10.1016/j.ijbiomac.2023.124942.

[40] T. Tadros, Colloid and interface aspects of pharmaceutical science, in: H. Ohshima, K.B.T.-C. and I.S. in P.R. and D. Makino (Eds.), Colloid and Interface Science in Pharmaceutical Research and Development, Elsevier, Amsterdam, 2014, pp. 29–54, https://doi.org/10.1016/B978-0-444-62614-1.00002-8.

[41] M. Božik, P. Nový, P. Klouček, Chemical composition and antimicrobial activity of cinnamon, thyme, oregano and clove essential oils against plant pathogenic Bacteria, Acta Univ. Agric. Silvic. Mendelianae Brun. 65 (2017) 1129–1134, https://doi.org/10.11118/actaun201765041129.

[42] C. Dallay, C. Malhiac, B. Duchemin, G. Savary, C. Picard, Effect of linalool on lamellar-structured emulsions: from molecular organization to organoleptic properties, Food Hydrocoll. 149 (2024) 109575, https://doi.org/10.1016/j.foodhyd.2023.109575.

[43] J.C. Courtenay, Y. Jin, J. Schmitt, K.M.Z. Hossain, N. Mahmoudi, K.J. Edler, J. L. Scott, Salt-responsive Pickering emulsions stabilized by functionalized cellulose nanofibrils, Langmuir 37 (2021) 6864–6873, https://doi.org/10.1021/acs.langmuir.0c03306.

[44] J.L. Sanchez-Salvador, A. Balea, M.C. Monte, A. Blanco, C. Negro, Pickering emulsions containing cellulose microfibers produced by mechanical treatments as stabilizer in the food industry, Appl. Sci. 9 (2019) 359, https://doi.org/10.3390/app9020359.

[45] A. Isogai, T. Saito, H. Fukuzumi, TEMPO-oxidized cellulose nanofibers, Nanoscale 3 (2011) 71–85, https://doi.org/10.1039/c0nr00583e.
[46] D.O. Abranches, M.A.R. Martins, L.P. Silva, N. Schaeffer, S.P. Pinho, J.A. P. Coutinho, Phenolic hydrogen bond donors in the formation of non-ionic deep eutectic solvents: the quest for type V DES, Chem. Commun. 55 (2019) 10253–10256, https://doi.org/10.1039/C9CC04846D.
[47] A.J. de Jesus, H. Yin, 5.14- supramolecular membrane chemistry, in: J.L.B.T.-C.S.C. I.I. Atwood (Ed.), Comprehensive Supramolecular Chemistry II, Elsevier, Oxford, 2017, pp. 311–328, https://doi.org/10.1016/B978-0-12-409547-2.12572-7.
[48] Y. Du, J. Liu, J. Wang, B. Wang, H. Li, Y. Su, Starch-based bio-latex redistribution during paper coating consolidation, Prog. Org. Coat. 106 (2017) 155–162.
[49] I. Filipova, F. Serra, Q. Tarrés, P. Mutjé, M. Delgado-Aguilar, Oxidative treatments for cellulose nanofibers production: a comparative study between TEMPO-mediated and ammonium persulfate oxidation, Cellulose 27 (2020) 10671–10688, https://doi.org/10.1007/s10570-020-03089-7.
[50] E.B. Heggset, R. Aaen, T. Veslum, M. Henriksson, S. Simon, K. Syverud, Cellulose nanofibrils as rheology modifier in mayonnaise – a pilot scale demonstration, Food Hydrocoll. 108 (2020), https://doi.org/10.1016/j.foodhyd.2020.106084.
[51] R. Darby, Pressure drop for non-Newtonian slurries : a wider path, Chem. Eng. 107 (2000) 64–67.
[52] M.A. Hubbe, P. Tayeb, M. Joyce, P. Tyagi, M. Kehoe, K. Dimic-Misic, L. Pal, Rheology of nanocellulose-rich aqueous suspensions: a review, Bioresources 12 (2017) 9556–9661, https://doi.org/10.15376/biores.12.4.Hubbe.
[53] N.O. Mishchuk, Chapter 9-coalescence kinetics of Brownian emulsions, in: D.N.B. T.-I.S. and T. Petsev (Ed.), Emulsions: Structure Stability and Interactions, Elsevier, 2004, pp. 351–390, https://doi.org/10.1016/S1573-4285(04)80011-5.
[54] P. Tyagi, L.A. Lucia, M.A. Hubbe, L. Pal, Nanocellulose-based multilayer barrier coatings for gas, oil, and grease resistance, Carbohydr. Polym. 206 (2019) 281–288.
[55] Q. Tarrés, H. Oliver-Ortega, P.J. Ferreira, M.À. Pèlach, P. Mutjé, M. Delgado-Aguilar, Towards a new generation of functional fiber-based packaging: cellulose nanofibers for improved barrier, mechanical and surface properties, Cellulose 25 (2018) 683–695, https://doi.org/10.1007/s10570-017-1572-7.
[56] Z. Rui, D. Yu, F. Zhang, Novel cellulose nanocrystal/metal-organic framework composites: transforming ASA-sized cellulose paper for innovative food packaging solutions, Ind Crops Prod 207 (2024) 117771, https://doi.org/10.1016/j.indcrop.2023.117771.
[57] E.C. Lengowski, E.A. Bonfatti Júnior, L. Simon, G.I.B. de Muñiz, A.S. de Andrade, S. Nisgoski, U. Klock, Different degree of fibrillation: strategy to reduce permeability in nanocellulose-starch films, Cellulose 27 (2020) 10855–10872, https://doi.org/10.1007/s10570-020-03232-4.
[58] Y. Montero, A.G. Souza, É.R. Oliveira, D. dos Santos Rosa, Nanocellulose functionalized with cinnamon essential oil: a potential application in active biodegradable packaging for strawberry, sustainable, Mater. Technol. 29 (2021) e00289, https://doi.org/10.1016/j.susmat.2021.e00289.
[59] S. De-Montijo-Prieto, M.D. Razola-Díaz, A.M. Gómez-Caravaca, E.J. Guerra-Hernandez, M. Jiménez-Valera, B. Garcia-Villanova, A. Ruiz-Bravo, V. Verardo, Essential oils from fruit and vegetables, aromatic herbs, and spices: composition, antioxidant, and antimicrobial activities, Biology (Basel) 10 (2021) 1091, https://doi.org/10.3390/biology10111091.
[60] Y. Niu, Y. Gao, Z. Xiao, C. Mao, H. Wang, Y. Geng, Y. Ye, X. Kou, Preparation and characterisation of linalool oil-in-water starch-based Pickering emulsions and the effects of the addition of cellulose nanocrystals on their stability, Int. J. Biol. Macromol. 247 (2023) 125732, https://doi.org/10.1016/j.ijbiomac.2023.125732.
[61] European Commission, EU Lists of Flavourings. https://food.ec.europa.eu/safety/food-improvement-agents/flavourings/eu-lists-flavourings_en, 2023. (Accessed 27 July 2023).
[62] Y. Wen, J. Liu, L. Jiang, Z. Zhu, S. He, S. He, W. Shao, Development of intelligent/active food packaging film based on TEMPO-oxidized bacterial cellulose containing thymol and anthocyanin-rich purple potato extract for shelf life extension of shrimp, Food Packag. Shelf Life 29 (2021) 100709, https://doi.org/10.1016/j.fpsl.2021.100709.
[63] H. Miladi, T. Zmantar, B. Kouidhi, Y. Chaabouni, K. Mahdouani, A. Bakhrouf, K. Chaieb, Use of carvacrol, thymol, and eugenol for biofilm eradication and resistance modifying susceptibility of Salmonella enterica serovar Typhimurium strains to nalidixic acid, Microb. Pathog. 104 (2017) 56–63, https://doi.org/10.1016/j.micpath.2017.01.012.
[64] Y. Wang, K.L. Yam, Inhibitory effect of thymol via different modes of delivery on growth of Escherichia coli DH5α, food packag shelf, Life 16 (2018) 92–96, https://doi.org/10.1016/j.fpsl.2018.02.007.
[65] S. Min, R. Priyadarshi, P. Ezati, J.-W. Rhim, J.T. Kim, Chitosan-based multifunctional coating combined with sulfur quantum dots to prevent Listeria contamination of enoki mushrooms, Food Packag. Shelf Life 35 (2023) 101014, https://doi.org/10.1016/j.fpsl.2022.101014.
[66] M. Tiecco, A. Grillo, E. Mosconi, W. Kaiser, T. Del Giacco, R. Germani, Advances in the development of novel green liquids: thymol/water, thymol/urea and thymol/phenylacetic acid as innovative hydrophobic natural deep eutectic solvents, J. Mol. Liq. 364 (2022) 120043, https://doi.org/10.1016/j.molliq.2022.120043.
[67] R. Aguado, A.C.S. Ferreira, S. Gramacho, D. Murtinho, A.J.M. Valente, Crosslinking of Surface-Sizing Starch with Cyclodextrin Units Enhances the Performance of Paper as Essential Oil Carrier 37, 2022, pp. 413–421, https://doi.org/10.1515/npprj-2022-0034.